Egyptian Journal of Chemistry

http://ejchem.journals.ekb.eg/

Fabrication of novel green magnetic electrospun nanofibers based on Fe_3O_4 nanoparticles/PVA/chitosan/collagen

A. Abou-Okeil[1], R. Refaei1, E. M. Khalil[2], Sh. E. Moustafa[1], Hassan M. Ibrahim[1]*

[1]Pretreatment and Finishing of Cellulosic Fibers Dept., Textile Industries Research Division, National Research Centre, 33 El Bohouth st., Dokki, Cairo, Egypt, P.O.12622

[2]Chemistry Dept., Faculty of Science, Helwan University

Abstract

Herein iron oxide nanoparticles were successfully prepared from $FeCl_3 \cdot 6H_2O$ (1.1 g) and $FeCl_2 \cdot 4H_2O$ (0.4 g) by addition of ammonium hydroxide via coprecipitation method (CPC). The conditions for the preparation of IONPs were optimized. IONPs were characterized by transmission electron microscope (TEM) and vibrating sample magnetometer (VSM). Magnetic electrospun nanofibers based on Fe_3O_4 nanoparticles/PVA/chitosan/collagen were fabricated using an electrospinning technique. In the absence and presence of ciprofloxacin, nanofibers were made from Fe_3O_4 nanoparticles that made up around 10% of the polymers. The viscosity and conductivity of several composite polymer formulations were measured as critical metrics. The electrospun nanofibers were characterized by Fourier transformation infrared spectroscopy (ATR- FTIR) and scanning electron microscope (SEM). The diameter of the nanofibers, antibacterial capabilities, and magnetism of the nanofibers were all measured. Electrospun magnetic nanofibers with higher antibacterial activity and supermagnetism were produced. In addition, the use of ciprofloxacin antibiotics improved these qualities.

Keywords: novel green, magnetic electrospun nanofibers, Fe_3O_4 nanoparticles, polyvinyl alcohol, chitosan, collagen

1. Introduction

Nanotechnology has progressed to the point where it is now possible to produce, characterise, and customise the beneficial properties of nanoparticles for biomedical activities and diagnostics in the previous ten years. (1-4). Inorganic nanoparticles, which exist between the molecular and solid phases, combine chemical accessibility with bulk phase physical features. (5-7). As a result, they're perfect components for creating nanostructured materials and devices with variable physical and chemical properties (8-11).

Magnetic nanoparticles [MNPs] have physical and chemical capabilities that are not found in atoms or their bulk equivalents.(12). Because each particle can be seen as a single magnetic area, nanoscale measuring effects and the huge surface region of magnetic nanoparticles substantially alternate some of the magnetic properties and display superparamagnetic events and quantum tunnelling of magnetization. (13). Superparamagnetic nanoparticles have a high workability for a variety of biomedical applications due to their unique mesoscopic physical, chemical, thermal, and mechanical properties. (14-17), Tissue repair, drug administration, and magnetic resonance imaging (MRI) are just a few examples. Iron oxide nanoparticles (IONPs) are one of the most widely utilised nanoparticle formulations in biomedical applications due to their low toxicity, inexpensive manufacturing costs, and unique magnetic characteristics. (18-24). IONPs, in particular, were particularly efficient as MRI contrast agents in the imaging of the liver. (18, 25). In-vitro diagnostics using tiny iron oxide particles has been conducted for

*Corresponding author e-mail: hmaibrahim@gmail.com.; (Hassan M. Ibrahim).
Receive Date: 03 December 2021, Revise Date: 26 December 2021, Accept Date: 03 January 2022
DOI: 10.21608/ejchem.2022.109235.4980

nearly 40 years. (26). Previously, more research was done with a variety of iron oxides in the area of nanosized magnetic particles (mostly maghemite, g-Fe_2O_3, or magnetite, Fe_3O_4, single domains of about 5–20 nm in diameter), with magnetite being a particularly promising candidate because its biocompatibility has already been established. (27). Researchers have shown an increased interest in multifunctional nanomaterials that are intended for use in therapeutics and diagnostics applications in recent decades (28-33). Iron oxide magnetic nanoparticles (IONPs) are gaining popularity in a variety of sectors, including physics, medicine, biology, and materials science. (34-36) because of their multifunctional properties, such as small size, magnetic susceptibility, biocompatibility, low toxicity, stability, the ability to modify surfaces, and the ability to be readily controlled with the use of an external magnetic field (37, 38). The surface coating and precise modification of IONPs is the most significant requirement for their successful use in technical and biological applications. (39, 40).

Electrospinning is a simple and effective method for making nanofibers. (41). Electrospinning of natural polymers has recently exploded in popularity, owing to natural polymers' superior biocompatibility and biodegradability, as well as their suitability for the human body over manufactured choices. (42, 43). Many biopolymers, such as chitosan, have been successfully manufactured into nanofibers. (44, 45), collagen/silk (46), keratin/fibroin (47), hyaluronic acid (48), gelatin (49), and cellulose derivatives (50) using this technique. In the biomedical field, electrospun polymeric fibres play a significant role. Due to the wide range of applications, such as DNA separation, the fabrication of magnetic nanofibers that are sensitive to changes in the external magnetic field is amazing in the field of nanotechnology. (51), targeting drug delivery (52-55), bone tissue engineering (56) and microwave absorption (57). Magnetic nanoparticles can be incorporated into biopolymers to improve their biomedical uses. Superparamagnetic nanoparticles have several advantages for making this nano-composite, including ease of training and functionalization, minimal toxicity, and low cost. (58, 59). Because of its unique magnetic properties and minimal toxicity, iron oxide (-Fe_2O_3 or Fe_3O_4) is the most trustworthy of the magnetic nanoparticles. Because of its superparamagnetism under 20 nm and natural organic compatibility, magnetite (Fe_3O_4) was previously intensively explored and exploited in organic applications such as magnetic resonance imaging (MRI), drug delivery, biosensor, magnetic separation, and clinical prognosis. (60). The Fe_3O_4 nanoparticles must be chemically stable, homogenous in size, and well-dispersed in liquid media, ideally water, for the majority of these applications. However, widespread agglomeration of magnetic nanoparticles, particularly in electrospinning composite nanofibers, is a significant challenge in the manufacture of such nanocomposite. Some of the magnetic nanofibers were made by mixing dry Fe_3O_4 magnetic powder into the polymer solution and electrospinning them into magnetic nanofibers. (61, 62). However, obtaining homogenous dispersions of magnetic nanoparticles/polymer is difficult. This aggregation of Fe_3O_4 nanoparticles could be avoided by improving or covering the magnetite's floor with stabilisers such organic ligands. (63, 64) or steric polymer (65). However, pH sensitivity, a lack of functional groups, and a lack of consistency in the received suspensions limit the use of stabilisers. As a result, more magnetite/polymer combinations attract focal points.

In this work, we have successfully fabricated magnetic electrospun nanofibers based on Fe_3O_4 nanoparticles/PVA/chitosan/collagen using an electrospinning technique with Fe_3O_4 nanoparticles of about 10 wt. % of polymers in the absence and presence of ciprofloxacin antibiotic. The different composite polymers formulations were studied with measuring viscosity and conductivity as important parameters. The prepared fibres were evaluated by measuring fibres diameter, antibacterial properties, and also magnetism.

2. Methods

2.1. Materials

$FeCl_3 \cdot 6H_2O$ and $FeCl_2 \cdot 4H_2O$ were purchased from Merck (Darmstadt, Germany). NaOH (25 wt % in water). polyvinyl alcohol (PVA)-Oxford. Chitosan of medium molecular weight (MMW, 480 000 Da) and degree of deacetylation of 79.0% (Alfa Aesar Company). Ciprofloxacin hydrochloride was purchased from Fisher Company and used without further purification. All other chemicals and solvents were from general laboratory-grade chemicals. All

other chemicals were used at analytical grade without any purifications. Collagen was obtained from young rat tail tendons, according to the procedure described earlier (66). Tendons were washed in distilled water and dissolved in 0.1 M acetic acid for three days in 4 °C, the undissolved parts were removed by centrifugation for 10 min at 10 000 rpm. The completely frozen mixtures were lyophilized at - 55 °C and 5 Pa for 48 h (ALPHA 1–2 LD plus, CHRIST, Germany).

2.2. Synthesis of iron oxide nanoparticles [IONPs]

An aqueous solution (150 mL in deionized water) of $FeCl_3 \cdot 6H_2O$ (1.1 g) and $FeCl_2 \cdot 4H_2O$ (0.4 g), in the molar ratio 2Fe (III): 1Fe (II) prepared and kept at a constant temperature of 60 ◦C for 15 min under vigorous stirring. Then under vigorous stirring and N_2 gas, a solution of ammonium hydroxide (20 mL of NaOH (25 wt. %)) was added till the pH was reached ∼11 at which a black suspension was formed. This suspension was then stirred at 50 ºC for 2 h, under vigorous stirring and N_2 gas. IONPs were separated from the aqueous solution by an external magnet, washed with deionized water several times then dried in a vacuum oven overnight.

2.3. Electrospinning process

2.3.1 Preparation of electrospinning solution

The desired amount of polymers used, according to the concentration required was weighed. 1 % solution of chitosan (in 1% acetic acid), 1 % collagen (in 1% acetic acid), and 15 % PVA (in hot water) solutions were mixed with different volume ratios and the air bubbles were removed by sonication. After mixing, the electrospinning solutions were fed into 5-ml syringes with a metal end needle (22 gauges) and then mounted in a programmable syringe pump operated at 0.5 ml/h at 25 ± 2 °C. The positive lead from a high-voltage power generator was connected to the needle tip and a DC voltage of 17.5 kV was applied. The nanofibers were collected on an aluminium foil collector with a horizontal distance of 10 cm from the needle tip. In some experiments, A definite amount of IONPs and ciprofloxacin were added by suspension in a definite amount of distilled water to the polymer's mixture before electrospinning and mixed, the air bubbles were removed by sonification to prepare the nanofibers containing IONPs and/or ciprofloxacin antibiotic.

2.4. Testing and analysis

- Attenuated total reflection-Fourier transformation infrared, Infrared spectra were measured using high-resolution attenuated total reflection-Fourier transformation infrared spectroscopy (ATR-FTIR) (JASCO FT/IR-4700 spectrophotometer from Japan). The spectra were collected in the wavenumber range of 4000 to 400 cm^{-1}, resolution of 4 cm^{-1} with 2 mm/s scanning speed, and 1.0 cm^{-1} interval scanning using 64 repetitious scans on average.
- The magnetic properties of IONPs and electrospun magnetic nanofibers were studied with a vibrating sample magnetometer (VSM). The hysteresis loops of magnetic prepared IONPs and electrospun magnetic nanofibers were investigated by the VSM technique at 298 K
- The viscosity of the polymer solutions was determined by a rotation viscometer (Brookfield-DVBT) at room temperature.
- The electrical conductivity of the electro-spinning solutions was measured using a Myron L Ultra-meter II, Model 6P.
- Scanning electron microscope (SEM) images of the electrospun nanofibers of polymers blends were obtained using SEM Model Quanta 250 FEG (Field Emission Gun) attached with EDX Unit (Energy Dispersive X-Ray Analysis), with accelerating voltage 30 kV, magnification 14× up to 1,000,000, and resolution for Gun, FEI company, Netherlands". Samples were fixed to a sample holder and coated with a layer of gold in a vacuum using a sputter coater (S150A, Edwards, England) to produce a conductive surface. Gold-coated samples were placed in the microscope chamber. Features of sample morphology were obtained.
- Transmission electron microscope (TEM) was measured using Zeiss-EM10-Germany, operating at power 60 kV. TEM samples were prepared by dispersing 2–3 drops of NPs suspension on copper grids and dried at room temperature after removal of excess solution using a filter paper.
- The antibacterial activity against *Staphylococcus aureus (S. aureus)* as Gram-positive bacteria and *Escherichia coli (E. coli)* Gram-negative bacteria was evaluated by the bacterial colony counting

method (59), where a liquid culture was prepared by mixing 0.5 g peptone and 0.3 g beef extract in 100 ml water. 1 cm diameter of the crosslinked film samples was cut and put into 10 ml of liquid culture, to which 10 µl of microbe culture was added and the tested samples were then incubated for 24 h at 37°C. From each incubated sample, 100 µl of the solution was taken, diluted, and distributed onto an agar plate. All plates were subjected to incubation for 24 hrs. and the colonies formed were then, counted. The percentage reduction was determined as follows:

$$\%\ Reduction\ in\ CFU\ (Colony\ Forming\ Units) = (C - A)/C \times 100$$

Where, C and A are the colonies counted from the plate of the control and treated samples, respectively.

3. Results and discussion

3.1. Preparation of Fe_3O_4 magnetic nanoparticles

Fig. 1 shows the TEM image of prepared IONPs, it is clear from **Fig.** 1 (a) that the shape of IONPs was homogeneous and almost all particles were found to be semi-spherical. The particle dimension of IONPs was in the range of 15.01 nm – 17.2 nm **Fig 1** (b). It can be seen from the histogram that the particle size distribution of the prepared IONPs was in the range of 6 nm – 16 nm and the majority of particles were about 11 nm in size

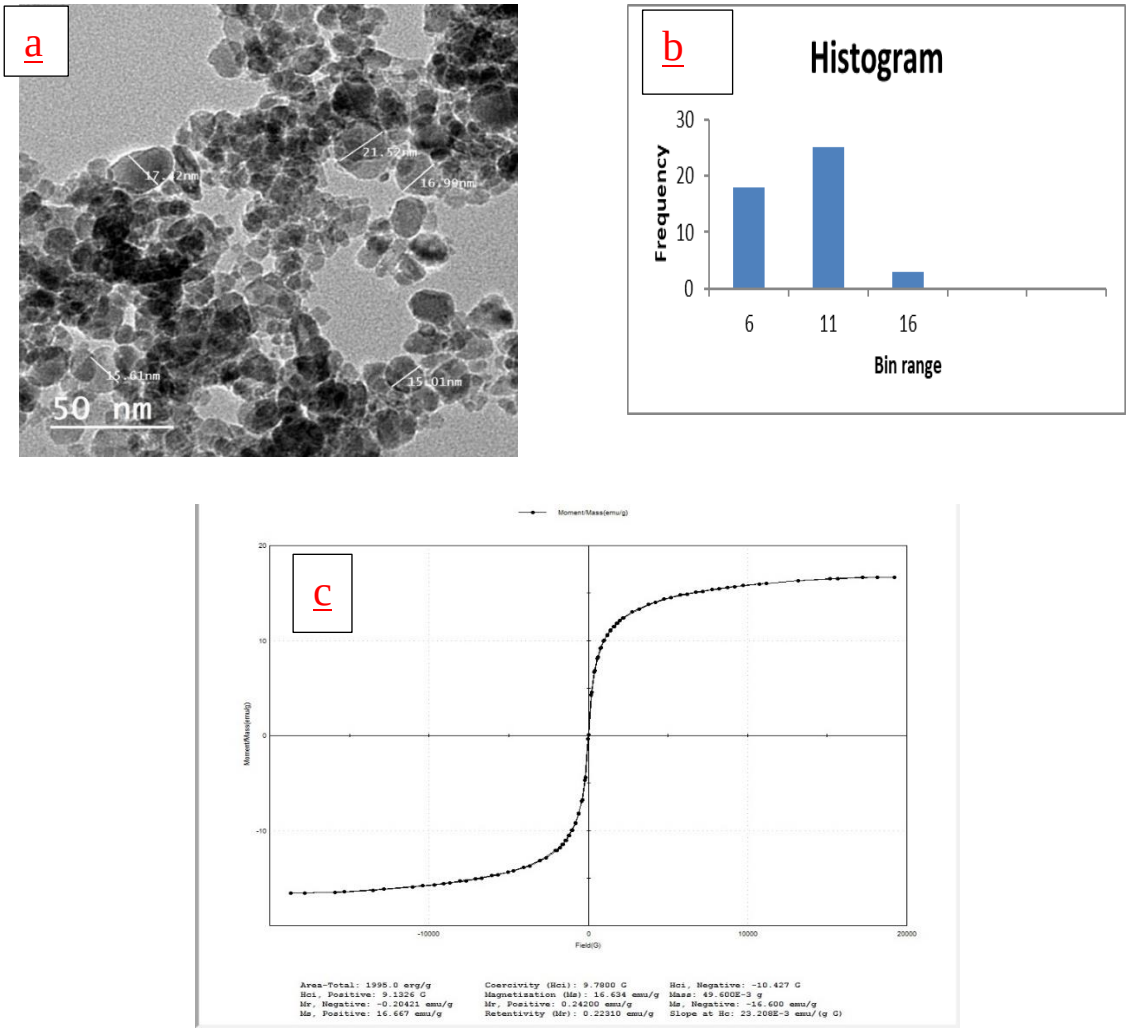

Fig. 1. TEM image (a), Histogram (b), and VSM curve (c) of IONPs

The hysteresis loop of the MNPs is shown in **Fig.** 1 (c) and is made using a vibrating sample magnetometer (VSM). The saturation magnetization and of the MNPs is about 16.6 emu/g and, indicating high saturation magnetization and superparamagnetic behaviour.

3.2. Fabrication of electrospun magnetic nanofibers

3.2.1. Effect of the polymers composition on fabricated magnetic nanofibers

In the present study composite from chitosan, collagen, and polyvinyl alcohol (PVA) were used to obtain fabricated nanofibers from an electrospinning device. PVA act as a fibre aiding polymer whereas chitosan and collagen were the active functional polymers in this composite. So, optimized was applied to study and obtain the best one for fibre formation and magnetic properties.

Table 1 shows the effect of polymers composition on the viscosity, conductivity, and nanofibers diameter. It's clear from Table 1 that increasing the amount of chitosan in the composite formulations has a reasonable effect on the viscosity of the electrospinning composite mixture. As shown in Table 1 that the viscosity of the electrospinning composite mixture was 115, 150.8, 190, 238 and 283.8 cP for collagen (formulation 1); chitosan/collagen, 0.42 (formulation 2); chitosan/collagen, 1 (formulation 3); chitosan/collagen, 2.3 (formulation 4) and chitosan (formulation 5) only respectively at PVA constant concentration. This holds due to the high viscosity of chitosan polymer along with the expected interaction between the polymers found in the electrospinning composite mixture. Also increasing the chitosan concentration leads to an enhancement in the conductivity of the electrospinning composite mixture. The conductivity of the electrospinning mixture was 1.168, 1.673, 2.38, 2.73, and 3.19 mS for collagen; chitosan/collagen, 0.42; chitosan/collagen, 2.3 and chitosan only respectively at PVA constant concentration. As the viscosity and the conductivity have an important effect on the quality of the electrospinning process as well as the diameter of the produced fibres. Table 1 showed that increasing the conductivity and viscosity of the electrospinning composite mixture had a remarkable effect on the fibre's diameter. As increasing chitosan concentration (increasing viscosity and conductivity) The majority of fibres diameters decreased. Table 1 revealed that the majority of fibres diameter is 120, 94, 99, 81, and 71 nm for collagen; chitosan/collagen, 0.42; chitosan/collagen, 2.3 and chitosan only respectively at PVA constant concentration. In a parallel experiment to examine the effect of PVA concentration on fibres diameter, it is shown in Table 1 that decreasing the amount of PVA added to electrospinning composite mixture (formulation 6) to half the amount used in the other formulation leads to increasing the diameter of the fibre to about 142 nm.

3.2.2. FTIR spectroscopy of electrospun nanofibers

Fig. 2 showed the FTIR spectrum of collagen, chitosan, PVA polymers, and the electrospun nanofibers prepared from electrospinning of a definite composition of these polymers. The characteristics peaks of pure collagen were shown as the peak of amide I band, stretching at 1628 cm^{-1}, amide II band, N-H deformation at 1549 $cm^{-1,}$ and amide A band, N-H stretching at 3291 cm^{-1}. Chitosan gave its known peaks of amide I band at 1625 cm^{-1}, amide II band at 1525 $cm^{-1,}$ and amide III bands at 1437 cm^{-1}. The own peaks of PVA were found at 3291, 2903, 1711, 1412, 1368, and 800 cm^{-1}, for O–H stretching vibration of the hydroxy group, CH_2 asymmetric stretching vibration, C=O carbonyl stretch, C–H bending vibration of CH_2, and C-C stretching vibration, accordingly (65, 67, 68).

Table 1. Properties of different electrospinning formulations

Formulation	Chitosan (1%)	Collagen (1%)	PVA (15%)	viscosity (cP) shear rate 100 (1/S)	conductivity (mS)	Average fibers diameter (nm)	Majority of fiber diameter (nm)
1	0 ml	10 ml	10 ml	115	1.168 mS	97.2 ± 49.3	120
2	3 ml	7 ml	10 ml	150.8	1.673 mS	167.46 ± 74	94
3	7 ml	3 ml	10 ml	238.1	2.73 mS	66.70 ± 27	81
4	5 ml	5 ml	10 ml	117	2.38 mS	89.98 ± 39.9	99
5	10 ml	0 ml	10 ml	283.8	3.19 mS	60.95 ± 17.78	71
6	7 ml	8 ml	5 ml	67.47	2.18 mS	154.2 ± 61	142

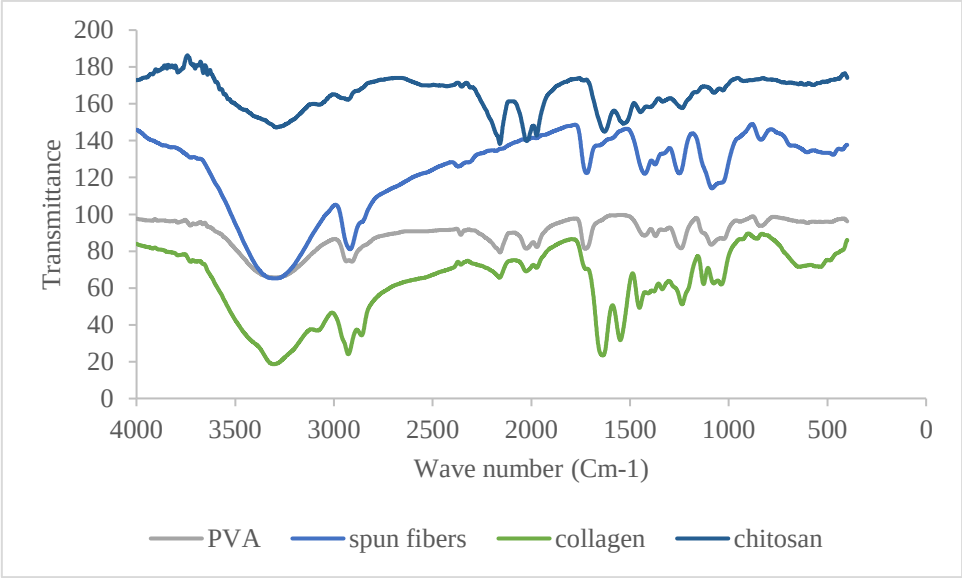

Fig. 2. FTIR of chitosan, collagen, and PVA Electrospun nanofibers and their components

Electrospun magnetic nanofibers showed the characteristic peaks of all the components of the electrospun composite polymers such as N-H stretching at 3291 cm^{-1} from collagen and chitosan, amide I band, stretching at 1628 cm^{-1}, amide II band, N-H deformation at 1549 cm^{-1} from collagen and chitosan. Also, CH_2 asymmetric stretching vibration at 2903 cm^{-1} from collagen, chitosan, and PVA. There is some shifting that can be attributed to the interaction between the functional groups of polymers components.

3.2.3. Scanning electron microscope (SEM) Images and histograms

SEM images of the prepared nanofibers are shown in **Fig.** 3. It can be seen from **Fig.** 3 that increasing the amount of chitosan in the electrospinning polymers composite formulations has a reasonable effect on the SEM images of the produced nanofibers. The SEM images of the produced nanofibers showed that the best SEM image was for formulation 2, that is the diameter of the fibre was homogeneous, and also the fibres had no beads. The SEM of the other formulations, 1, 3, 4, 5 showed almost homogeneous fibres diameter but with some beading. The histograms of the different formulations are shown in **Fig.** 4, it is shown that the majority of fibres diameters are 120, 94, 99, 81, and 71 nm for collagen; chitosan/collagen, 0.42; chitosan/collagen, 2.3 and chitosan only (Table 1) respectively at PVA constant concentration. So, from the SEM images and the histograms of fibres diameter, it can be seen that formulation 2 is the best one which gave fibres with a majority diameter of about 94 nm and homogeneous and beads free nanofibers.

3.2.4. Antibacterial activity of fabricated magnetic nanoparticles

Fig. 5 shows the antibacterial properties of the above-mentioned blend nanofibers expressed as the percent reduction of CFU of Gram-positive (*S. aureus*) and Gram-negative (*E. coli*) bacteria. The results depict that all obtained nanofibers samples showed high antibacterial activities. **Fig.** 5 shows that all prepared nanofibers have a high antibacterial property gains Gram-positive (S. aureus) and Gram-negative (E. coli) bacteria. The antibacterial properties of the so prepared nanofibers were in the range of 47 % to about 98 % for Gram-positive (*S. aureus*) and from about 62 % to 90 % for Gram-negative (*E. coli*). Increasing the amount of chitosan has an enhancement effect on the antibacterial properties for both Gram-positive (*S. aureus*) and Gram-negative (*E. coli*). The lowest antibacterial properties were noticed for collagen nanofibers alone (3.28 % and 15.14 for Gram-positive (*S. aureus*) and Gram-negative (*E. coli*) respectively.

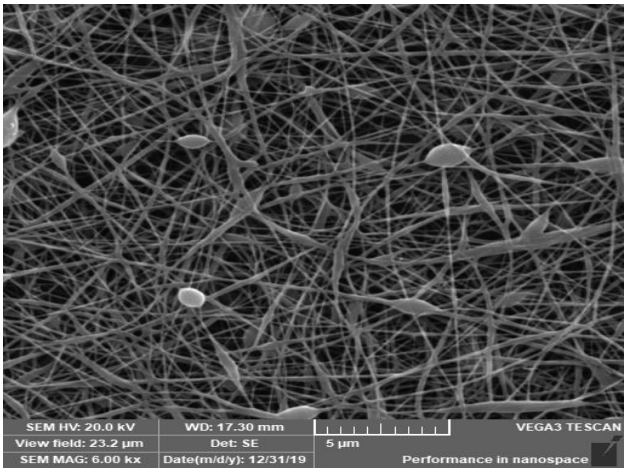

Formulation 1

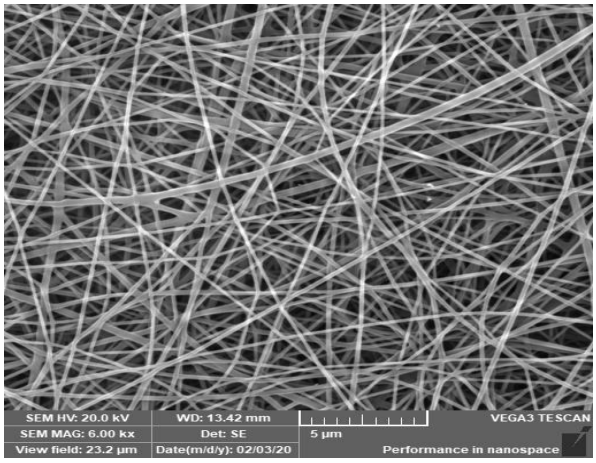

Formulation 2

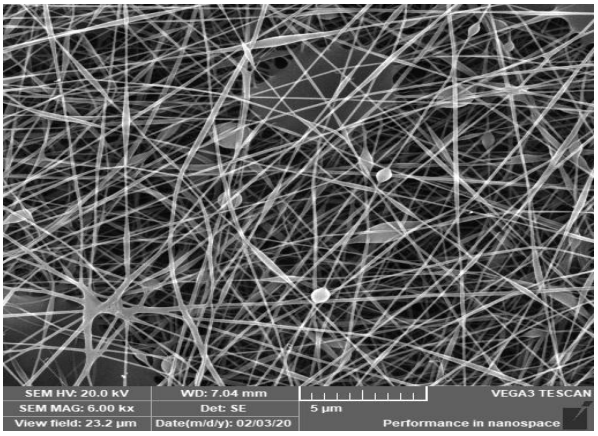

Formulation 3

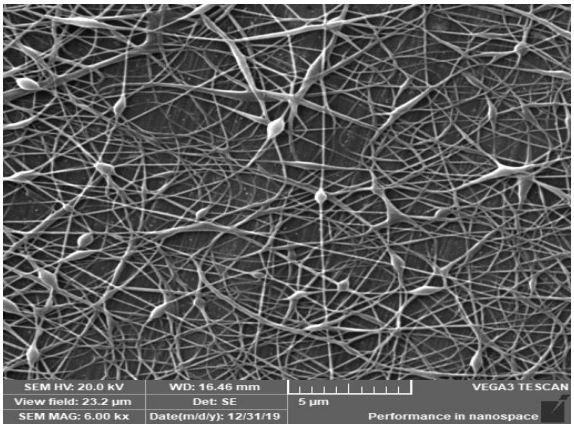

Formulation 4

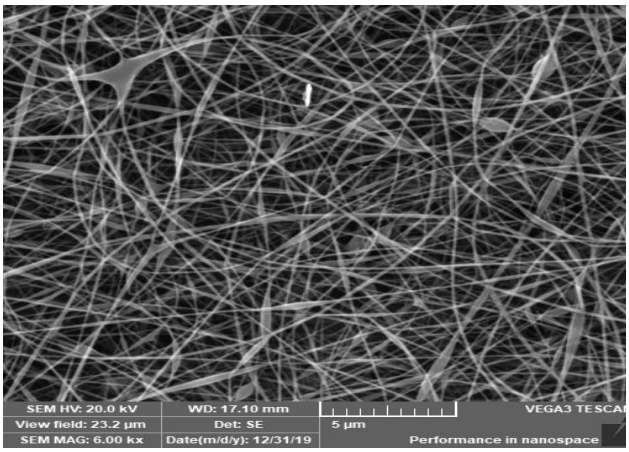

Formulation 5

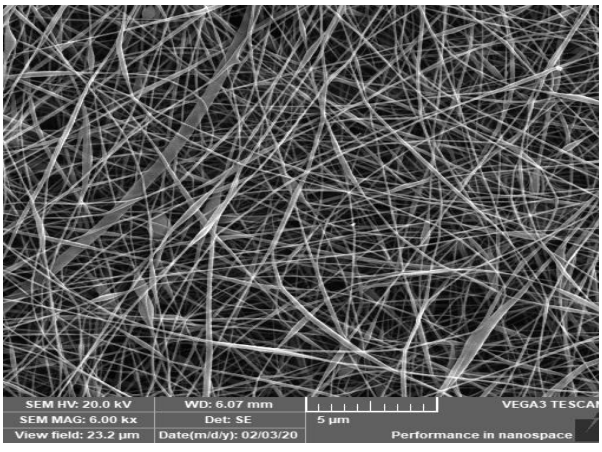

Formulation 6

Fig. 3. SEM Images of various formulations of the composite formed from chitosan, collagen, and PVA

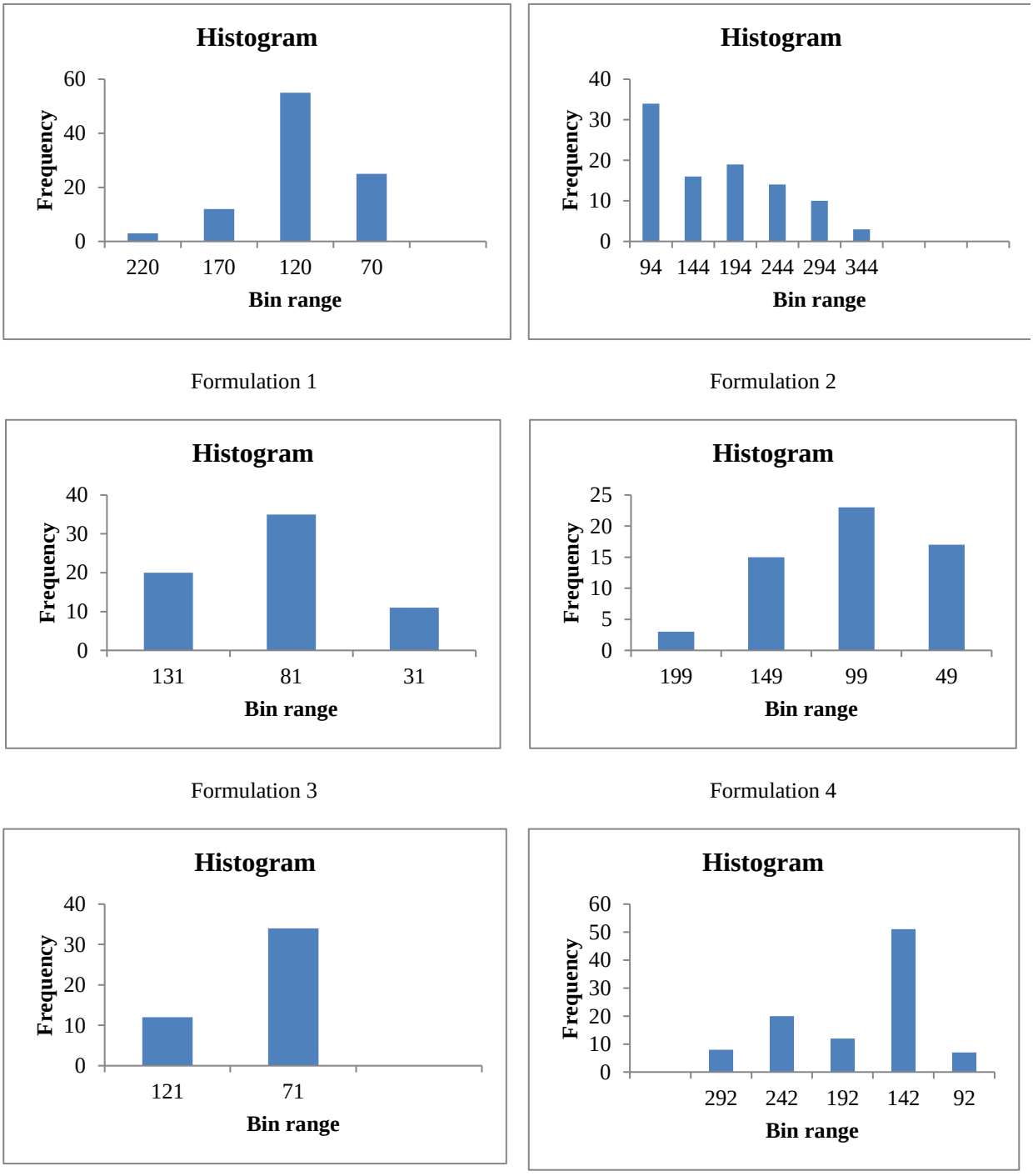

Fig. 4. Histograms of fibre diameter distribution curve of various formulations of the composite formed from chitosan, collagen, and PVA

3.3. Synthesis of Magnetic nanofibers in presence and absence of ciprofloxacin

Magnetic nanofibers were synthesized using formulation 2, that's A 10 % (based on the weight of polymers of IONPs and/or 0.001 mg ciprofloxacin were added by suspension in a definite amount of distilled water to the polymer's mixture (3 ml of 1 % chitosan; 7 ml of 1 % collagen and 10 ml of 15 % PVA) before electrospinning and mixed, the air bubbles were removed by sonification to prepare the nanofibers containing IONPs and/or ciprofloxacin. Table 2 and **Fig.** 6 showed the effect of added IONPs and/or ciprofloxacin on SEM images and also on the fibre's diameter and fibres diameter distribution. It is obvious from Table 2 and **Fig.** 6 that the fibres diameter was increased to about 249 nm and 221 nm for the nanofibers loaded with IONPs/ ciprofloxacin and the nanofibers loaded with ciprofloxacin alone compared to about 94 for the fibres without ciprofloxacin and/or IONPs (formulation 2, Table 1 and **Fig.** 4). This finding can be attributed to the effect of the magnetism of IONPs as well as to the dimension of the ciprofloxacin which may be affected the electrospinning process producing fibre with higher diameters. **Fig.** 6 revealed that the SEM images of the IOPNs and/or ciprofloxacin-loaded fibres. The SEM images showed beads-free and almost homogeneous fibres.

Sample 1. (0.16 gm MNP in 3ml H_2O added to the electrospinning formulation along with 0.001 gm ciprofloxacin into 2 ml H_2O); Sample 2. (0.001 gm ciprofloxacin into 2 ml H_2O added to the electrospinning formulation)

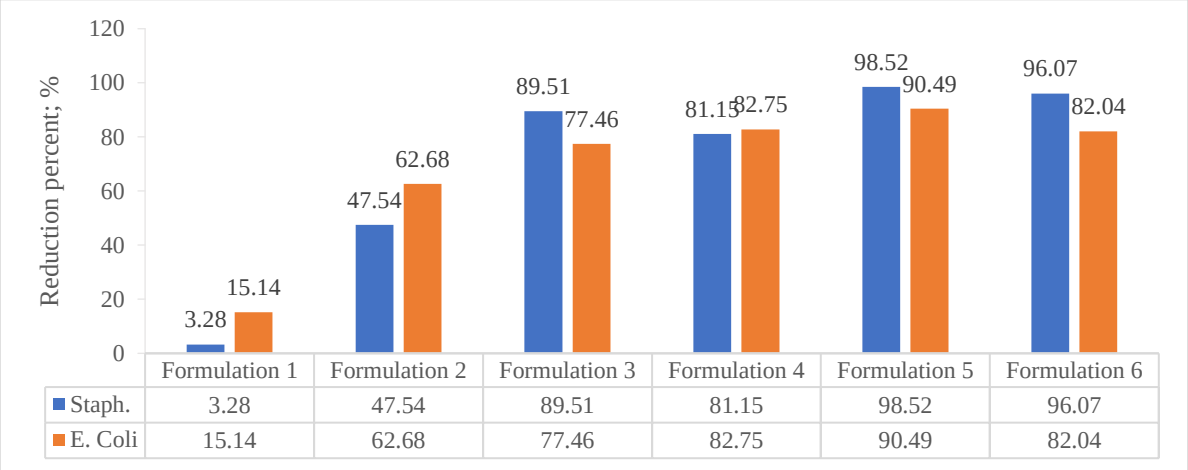

Fig. 5 Antibacterial activity of the electrospun nanofibers by bacterial colony count expressed in reduction percent

Table 2. Fibres diameter of electrospun nanofibers after adding IONPs and/or ciprofloxacin

Index	Chitosan (1%)	Collagen (1%)	PVA (15%)	Average fibers diameter (nm)	Majority fibers diameter (nm)
Formulation 2 with 10 % of IONPs (based on the weight of polymers) and 0.001 mg ciprofloxacin	3 ml	7 ml	10 ml	211.61 ± 62.12	249
Formulation 2 with ciprofloxacin	3 ml	7 ml	10 ml	165.83 ± 41.84	221

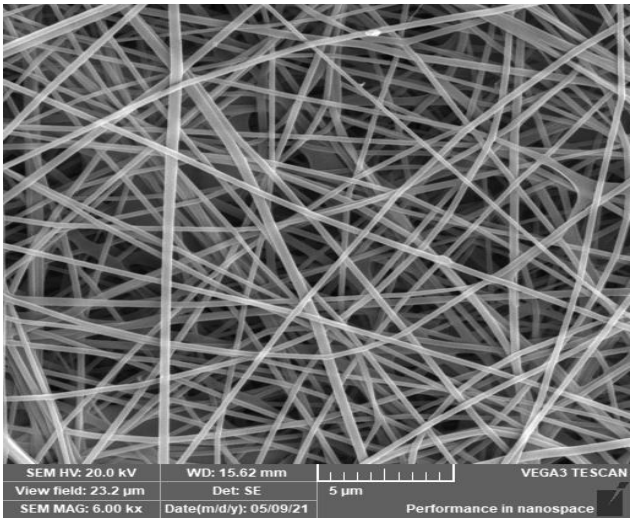

Formulation 2 with IONPs ciprofloxacin

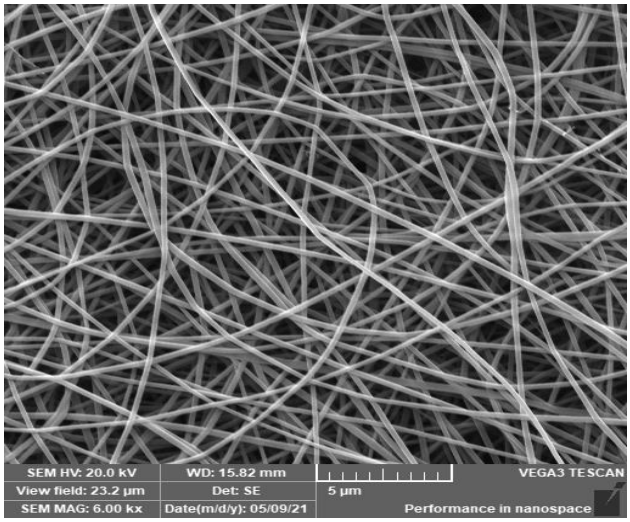

Formulation 2 with ciprofloxacin only

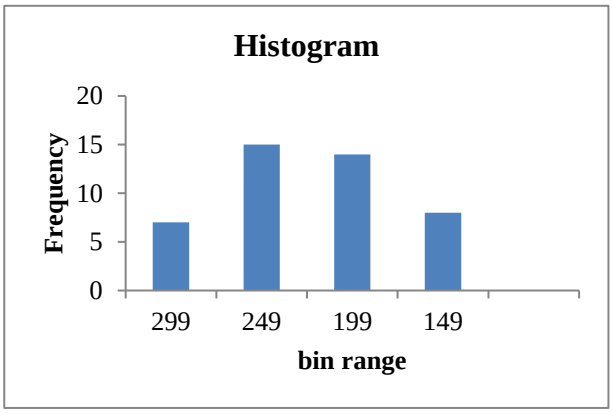

Formulation 2 with IONPs ciprofloxacin

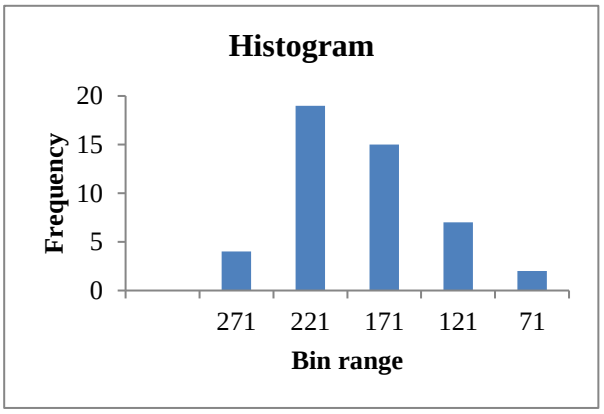

Formulation 2 with ciprofloxacin only

Fig. 6. SEM images and Histograms of nanofibres loaded with IOPNs and ciprofloxacin

3.3.1. Magnetic properties of synthesized nanofibers

The magnetic properties of synthesized nanofiber are studied by measuring magnetization as a function of field (**Fig.** 7). The magnetization was recorded in an applied magnetic field of $-20000 \leq H$ (Oe) ≤ 20000 at room temperature. The hysteresis loop of synthesized nanofiber is shown in **Fig.** 7, the saturation magnetization and of the synthesized nanofibers is about 0.16 emu/g.

3.3.2. Antibacterial Properties

Fig. 8 shows the antibacterial properties of the 10 % (based on the weight of polymers of IONPs and/or 0.001 mg ciprofloxacin loaded nanofibers using formulation 2 (3 ml of 1 % chitosan; 7 ml of 1 % collagen and 10 ml of 15 % PVA), compared to the antibacterial properties of nanofibers produced with formulation 2 only against. **Fig.** 8 depicted that adding IONPs and/or ciprofloxacin has an incremental effect on the antibacterial properties of the synthesized nanofibers expressed as the percent reduction of CFU of Gram-positive (*S. aureus*) and Gram-negative (*E. coli*) bacteria. The antibacterial properties of the IONPs/ ciprofloxacin loaded nanofibers, ciprofloxacin loaded nanofibers and nanofibers without ions and/or ciprofloxacin was found to be, 82 %, 89 % and 47 % against Gram-positive (*S. aureus*) respectively and 80 %, 92 % and 62 against Gram-negative (*E. coli*) bacteria respectively. This is leads us to say that IONPs and /or ciprofloxacin has increased the antibacterial properties which can be explained by the antibacterial effect of ciprofloxacin antibiotic and IONPs.

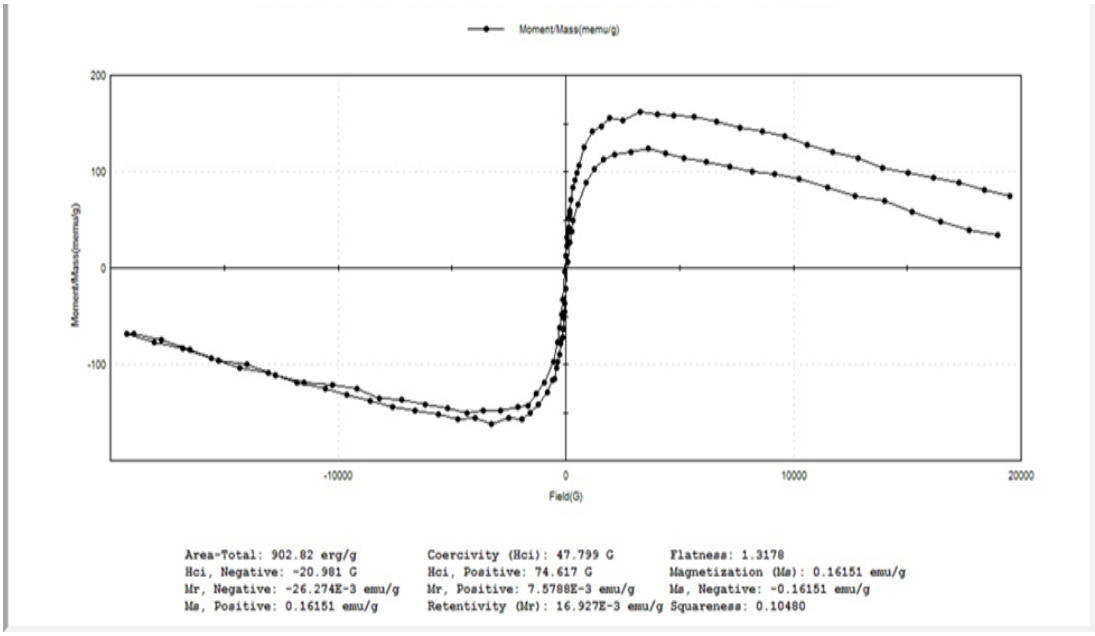

Fig. 7. VSM curve of nanofibres loaded with IOPNs and ciprofloxacin

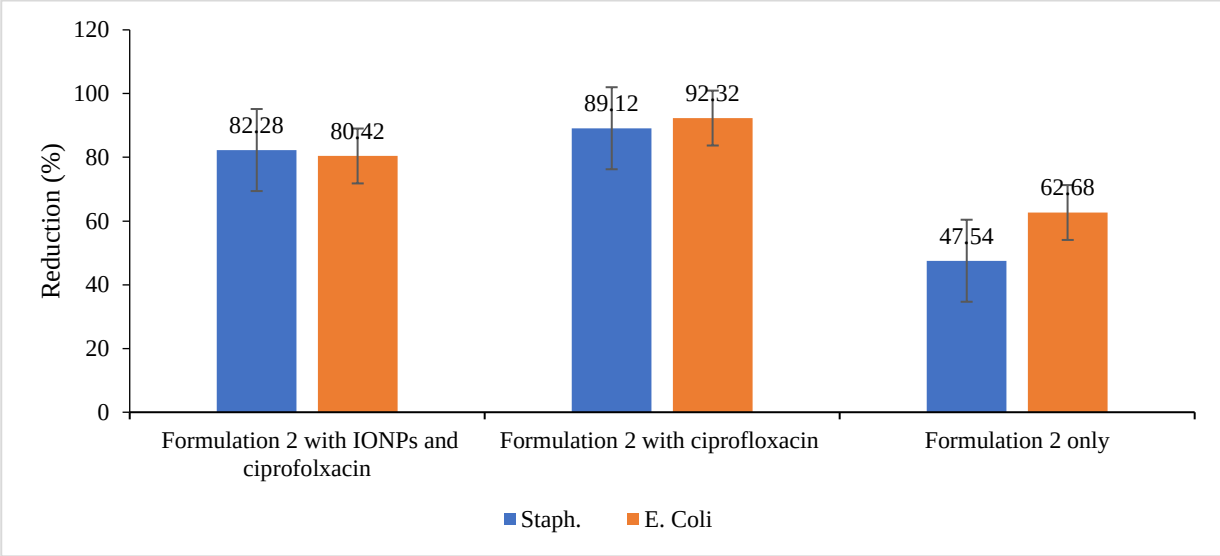

Fig. 8. Antibacterial activity against Gram-positive and Gram-negative bacteria expressed in bacterial reduction percent of nanofibres loaded with IOPNs and ciprofloxacin

4. Conclusion

Iron oxide nanoparticles (IONPs) with homogeneous hemispheres were made from ferric oxide. The size of the particles ranged from 15.1 to 17.2 nm. With a value of 16.6 emu/g, the synthesised IONPs have saturation magnetism and super magnetic behaviour. Electrospinning was used to make chitosan, collagen, and PVA polymers from magnetic nanofibers of various compositions. As the chitosan concentration in the composite increased the nanofiber diameter decreased whereas increasing of PVA concentration was accompanied by an increase in the fibre diameter (confirmed by SEM images). The fabricated nanofibers have antibacterial activity towards both Gram-positive and Gram-negative bacteria. Magnetic nanofibers were prepared from

formulation 2 (3:7:10; chitosan: collagen: PVA) due to it has fibres without any beads. Its fibre diameter increased by incorporation of ciprofloxacin antibiotic as shown from SEM images. In addition, the magnetism of the fabricated nanofibers was saturated with a 0.16 emu/g value. IONPs and /or ciprofloxacin have increased the antibacterial properties which can be explained by the antibacterial effect of ciprofloxacin antibiotics and IONPs.

5. References

1. Wilkinson JJMdt. Nanotechnology applications in medicine. 2003;14(5):29-31.
2. Panyam J, Labhasetwar VJAddr. Biodegradable nanoparticles for drug and gene delivery to cells and tissue. 2003;55(3):329-47.
3. Salama RM, Osman H, Ibrahim HM. Preparation of biocompatible chitosan nanoparticles loaded with Aloe vera extract for use as a novel drug delivery mechanism to improve the antibacterial characteristics of cellulose-based fabrics. Egyptian Journal of Chemistry. 2021.
4. Aly AA, Abou-Okeil A, Fahmy HM. Grafting of N-vinyl-2-pyrrolidone onto κ-carrageenan for silver nanoparticles synthesis. Carbohydrate Polymers. 2018;198:119-23.
5. Fahmy HM, Aly AA, Sayed SM, Abou-Okeil A. Κ-carrageenan/Na-alginate wound dressing with sustainable drug delivery properties. Polymers for Advanced Technologies. 2021;32(4):1793-801.
6. Nada AA, Soliman AAF, Aly AA, Abou-Okeil A. Stimuli-Free and Biocompatible Hydrogel via Hydrazone Chemistry: Synthesis, Characterization, and Bioassessment. Starch/Staerke. 2019;71(5-6).
7. Ibrahim NA, Kadry GA, Eid BM, Ibrahim HM. Enhanced antibacterial properties of polyester and polyacrylonitrile fabrics using Ag-Np dispersion/microwave treatment. AATCC Journal of Research. 2014;1(2):13-9.
8. Moghimi SM, Hunter AC, Murray JCJPr. Long-circulating and target-specific nanoparticles: theory to practice. 2001;53(2):283-318.
9. Ali MA, Bydoon E, Ibrahim HM. Bioactive Composite Nonwoven Surgical Dressing based on Cellulose Coated with Nanofiber Membrane using the layer-by-layer technique. Egyptian Journal of Chemistry. 2021.
10. Abdel-Mohdy FA, El-Bisi MK, Abou-Okeil A, Sleem AA, El-Sabbagh S, El-Shafei K, et al. Antimicrobial and haemostatic effect of chitosan/ polyacrylic acid hybrid membranes. Egyptian Journal of Chemistry. 2016;59(1):45-57.
11. Hakeim OA, Abou-Okeil A, Abdou LAW, Waly A. The influence of chitosan and some of its depolymerized grades on natural color printing. Journal of Applied Polymer Science. 2005;97(2):559-63.
12. Abou-Okeil A, Aly AA, Amr A, Soliman AAF. Biocompatible hydrogel for cartilage repair with adjustable properties. Polymers for Advanced Technologies. 2019;30(8):2026-33.
13. Goya G, Berquo T, Fonseca F, Morales MJJoap. Static and dynamic magnetic properties of spherical magnetite nanoparticles. 2003;94(5):3520-8.
14. Pankhurst QA, Connolly J, Jones SK, Dobson JJJopDAp. Applications of magnetic nanoparticles in biomedicine. 2003;36(13):R167.
15. Bakr MM, Taha MA, Osman H, Ibrahim HM. Novel green printing of cotton, wool and polyester fabrics with natural safflower dye nanoparticles. Egyptian Journal of Chemistry. 2021;64(11):6221-30.
16. El-Zawahry MM, Helmy HM, Abou-Okeil A. Enzymatic Treatment and Its Influence on Finishing and Dyeing Properties of Jute Fabrics. Research Journal of Textile and Apparel. 2009;13(4):34-44.
17. Abou-Okeil A, El-Shafie A, Hebeish A. Chitosan phosphate induced better thermal characteristics to cotton fabric. Journal of Applied Polymer Science. 2007;103(3):2021-6.
18. Wáng YXJ, Idée J-M. A comprehensive literatures update of clinical researches of superparamagnetic resonance iron oxide nanoparticles for magnetic resonance imaging. Quant Imaging Med Surg. 2017;7(1):88-122.
19. Lunov O, Uzhytchak M, Smolková B, Lunova M, Jirsa M, Dempsey NM, et al. Remote Actuation of Apoptosis in Liver Cancer Cells via Magneto-Mechanical Modulation of Iron Oxide Nanoparticles. 2019;11(12):1873.
20. Tong S, Zhu H, Bao G. Magnetic iron oxide nanoparticles for disease detection and therapy. Materials Today. 2019;31:86-99.
21. Mosaad RM, Samir A, Ibrahim HM. Median lethal dose (LD50) and cytotoxicity of Adriamycin in female albino mice. Journal of Applied Pharmaceutical Science. 2017;7(3):77-80.
22. Ibrahim HM, Saad MM, Aly NM. Preparation of single layer nonwoven fabric treated with chitosan nanoparticles and its utilization in gas filtration. International Journal of ChemTech Research. 2016;9(6):1-16.
23. Ibrahim H, El- Zairy EMR, Emam EAM, Adel E. Combined antimicrobial finishing dyeing

properties of cotton, polyester fabrics and their blends with acid and disperse dyes. Egyptian Journal of Chemistry. 2019;62(5):965-76.
24. Farag S, Ibrahim HM, Amr A, Asker MS, El-Shafai A. Preparation and characterization of ion exchanger based on bacterial cellulose for heavy metal cation removal. Egyptian Journal of Chemistry. 2019;62:457-66.
25. Wang Y-XJ. Superparamagnetic iron oxide based MRI contrast agents: Current status of clinical application. Quant Imaging Med Surg. 2011;1(1):35-40.
26. Gilchrist R, Medal R, Shorey WD, Hanselman RC, Parrott JC, Taylor CBJAos. Selective inductive heating of lymph nodes. 1957;146(4):596.
27. Schwertmann U, Cornell RM. Iron oxides in the laboratory: preparation and characterization: John Wiley & Sons; 2008.
28. Danafar H, Manjili H, Najafi MJDr. Study of copolymer composition on drug loading efficiency of enalapril in polymersomes and cytotoxicity of drug loaded nanoparticles. 2016;66(09):495-504.
29. Elmowafy EM, Tiboni M, Soliman MEJJoPI. Biocompatibility, biodegradation and biomedical applications of poly (lactic acid)/poly (lactic-co-glycolic acid) micro and nanoparticles. 2019;49(4):347-80.
30. Wang R, Shou D, Lv O, Kong Y, Deng L, Shen JJIjobm. pH-Controlled drug delivery with hybrid aerogel of chitosan, carboxymethyl cellulose and graphene oxide as the carrier. 2017;103:248-53.
31. Danafar H, Rostamizadeh K, Davaran S, Hamidi MJDd, pharmacy i. Co-delivery of hydrophilic and hydrophobic drugs by micelles: a new approach using drug conjugated PEG–PCLNanoparticles. 2017;43(11):1908-18.
32. Hashem A, Okeil A, Fikry M, Aly A, Aniagor CO. Isotherm and Kinetics Parametric Studies for Aqueous Hg(II) Uptake onto N-[2-(Methylamino)Ethyl]Ethane-1,2-Diaminated Acrylic Fibre. Arabian Journal for Science and Engineering. 2021;46(7):6703-14.
33. Ibrahim HM, Aly AA, Taha GM, El-Alfy EA. Production of antibacterial cotton fabrics via green treatment with nontoxic natural biopolymer gelatin. Egyptian Journal of Chemistry. 2020;63:655-96.
34. Shaabani A, Nosrati H, Seyyedhamzeh MJRoCI. Cellulose@ Fe 2 O 3 nanoparticle composites: magnetically recyclable nanocatalyst for the synthesis of 3-aminoimidazo [1, 2-a] pyridines. 2015;41(6):3719-27.
35. Aliabadi M, Shagholani HJIjobm. Synthesis of a novel biocompatible nanocomposite of graphene oxide and magnetic nanoparticles for drug delivery. 2017;98:287-91.
36. Abdel Sayed NI, El Badry K, Abdel Mohsen HM. Conductimetric studies of charge transfer complexes of p-Chloranil with some alicyclic amines in polar media. Journal of the Chinese Chemical Society. 2003;50(2):193-9.
37. Atacan K, Çakıroğlu B, Özacar MJIjobm. Covalent immobilization of trypsin onto modified magnetite nanoparticles and its application for casein digestion. 2017;97:148-55.
38. Arias JL, Reddy LH, Othman M, Gillet B, Desmaele D, Zouhiri F, et al. Squalene based nanocomposites: a new platform for the design of multifunctional pharmaceutical theragnostics. 2011;5(2):1513-21.
39. Wu Z, Yang S, Wu WJN. Shape control of inorganic nanoparticles from solution. 2016;8(3):1237-59.
40. Nosrati H, Salehiabar M, Attari E, Davaran S, Danafar H, Manjili HKJAOC. Green and one-pot surface coating of iron oxide magnetic nanoparticles with natural amino acids and biocompatibility investigation. 2018;32(2):e4069.
41. Greiner A, Wendorff JHJACIE. Cover picture: electrospinning: a fascinating method for the preparation of ultrathin fibers (Angew. Chem. Int. Ed. 30/2007). 2007;46(30):5633-.
42. Nawalakhe R, Shi Q, Vitchuli N, Noar J, Caldwell JM, Breidt F, et al. Novel atmospheric plasma enhanced chitosan nanofiber/gauze composite wound dressings. 2013;129(2):916-23.
43. Abou-Okeil A, Fahmy HM, Fouda MMG, Aly AA, Ibrahim HM. Hyaluronic Acid/Oxidized K-Carrageenan Electrospun Nanofibers Synthesis and Antibacterial Properties. BioNanoScience. 2021;11(3):687-95.
44. Ignatova M, Manolova N, Rashkov IJMb. Electrospun Antibacterial Chitosan-B ased Fibers. 2013;13(7):860-72.
45. Cooper A, Jana S, Bhattarai N, Zhang MJJomc. Aligned chitosan-based nanofibers for enhanced myogenesis. 2010;20(40):8904-11.
46. Matthews JA, Wnek GE, Simpson DG, Bowlin GLJB. Electrospinning of collagen nanofibers. 2002;3(2):232-8.
47. Zoccola M, Aluigi A, Vineis C, Tonin C, Ferrero F, Piacentino MGJB. Study on cast membranes and electrospun nanofibers made from keratin/fibroin blends. 2008;9(10):2819-25.
48. Uppal R, Ramaswamy GN, Arnold C, Goodband R, Wang YJJoBMRPBAB. Hyaluronic acid nanofiber wound dressing—

production, characterization, and in vivo behavior. 2011;97(1):20-9.
49. Lu A, Zhu J, Zhang G, Sun GJJoMC. Gelatin nanofibers fabricated by extruding immiscible polymer solution blend and their application in tissue engineering. 2011;21(46):18674-80.
50. Aly AS, Abdel-Mohsen AM, Hrdina R, Abou-Okeil A. Preparation and characterization of polyethylene glycol/dimethyl siloxane adduct and its utilization as finishing agent for cotton fabric. Journal of Natural Fibers. 2011;8(3):176-88.
51. Xiang J, Shen X, Song F, Liu MJJoSSC. One-dimensional NiCuZn ferrite nanostructures: fabrication, structure, and magnetic properties. 2010;183(6):1239-44.
52. Lv G, He F, Wang X, Gao F, Zhang G, Wang T, et al. Novel nanocomposite of nano Fe3O4 and polylactide nanofibers for application in drug uptake and induction of cell death of leukemia cancer cells. 2008;24(5):2151-6.
53. Wang S, Sun Z, Yan E, Yuan J, Gao Y, Bai Y, et al. Magnetic composite nanofibers fabricated by electrospinning of Fe3O4/gelatin aqueous solutions. 2014;190:126-32.
54. Farag S, Asker MMS, Mahmoud MG, Ibrahim H, Amr A. Comparative study for bacterial cellulose production Using Egyptian Achromobacter sp. Research Journal of Pharmaceutical, Biological and Chemical Sciences. 2016;7(6):954-69.
55. Farag S, Ibrahim HM, Asker MS, Amr A, El-Shafaee A. Impregnation of silver nanoparticles into bacterial cellulose: Green synthesis and cytotoxicity. International Journal of ChemTech Research. 2015;8(12):651-61.
56. Meng J, Zhang Y, Qi X, Kong H, Wang C, Xu Z, et al. Paramagnetic nanofibrous composite films enhance the osteogenic responses of pre-osteoblast cells. 2010;2(12):2565-9.
57. Zhang T, Huang D, Yang Y, Kang F, Gu JJMS, B E. Fe3O4/carbon composite nanofiber absorber with enhanced microwave absorption performance. 2013;178(1):1-9.
58. Liao Y, He L, Huang J, Zhang J, Zhuang L, Shen H, et al. Magnetite nanoparticle-supported coordination polymer nanofibers: synthesis and catalytic application in Suzuki-Miyaura coupling. 2010;2(8):2333-8.
59. Ibrahim HM, Zaghloul S, Hashem M, El-Shafei A. A green approach to improve the antibacterial properties of cellulose based fabrics using Moringa oleifera extract in presence of silver nanoparticles. Cellulose. 2021;28(1):549-64.
60. Ho C-H, Tsai C-P, Chung C-C, Tsai C-Y, Chen F-R, Lin H-J, et al. Shape-controlled growth and shape-dependent cation site occupancy of monodisperse Fe3O4 nanoparticles. 2011;23(7):1753-60.
61. Guo J, Ye X, Liu W, Wu Q, Shen H, Shu KJML. Preparation and characterization of poly (acrylonitrile-co-acrylic acid) nanofibrous composites with Fe3O4 magnetic nanoparticles. 2009;63(15):1326-8.
62. Bayat M, Yang H, Ko FJP. Electromagnetic properties of electrospun Fe3O4/carbon composite nanofibers. 2011;52(7):1645-53.
63. Wan J, Yao Y, Tang GJAPA. Controlled-synthesis, characterization, and magnetic properties of Fe 3 O 4 nanostructures. 2007;89(2):529-32.
64. Xuan S, Wang Y-XJ, Yu JC, Cham-Fai Leung KJCoM. Tuning the grain size and particle size of superparamagnetic Fe3O4 microparticles. 2009;21(21):5079-87.
65. Lee J, Isobe T, Senna MJJoC, Science I. Preparation of Ultrafine Fe3O4Particles by Precipitation in the Presence of PVA at High pH. 1996;177(2):490-4.
66. Sionkowska A, Lewandowska K, Michalska M, Walczak M. Characterization of silk fibroin 3D composites modified by collagen. Journal of Molecular Liquids. 2016;215:323-7.
67. Bhat N, Nate M, Kurup M, Bambole V, Sabharwal SJNI, Materials MiPRSBBIw, et al. Effect of γ-radiation on the structure and morphology of polyvinyl alcohol films. 2005;237(3-4):585-92.
68. Omkaram I, Chakradhar RS, Rao JLJPBCM. EPR, optical, infrared and Raman studies of VO2+ ions in polyvinylalcohol films. 2007;388(1-2):318-25.